Biophysical Journal Volume 74 May 1998 2434–2442

Intramembrane Molecular Dipoles Affect the Membrane Insertion and Folding of a Model Amphiphilic Peptide

Josep Cladera and Paul O'Shea
The Welsh School of Pharmacy, Cardiff University, Cardiff CF1 3XF, Wales

ABSTRACT The relationship between the dipole potential and the interaction of the mitochondrial amphipathic signal sequence known as p25 with model membranes has been studied using 1-(3-sulfonatopropyl)-4-[β[2-(di-n-octyl-amino)-6-naphthyl]vinyl] pyridinium betaine (di-8-ANEPPS) as a fluorescent probe. The dipole potential of phosphatidylcholine membranes was modified by incorporating into the bilayer the sterols phloretin and 6-ketocholestanol (KC), which decrease and increase the dipole potential, respectively. The results derived from the application of a dual-wavelength ratiometric fluorescence method for following the variation of the membrane dipole potential have shown that when p25 inserts into the lipidic bilayer, a decrease in the dipole potential takes place. The magnitude of this decrease depends on the initial value of the dipole potential, i.e., before interaction with the peptide. Thus, when KC was incorporated into the bilayer, the decrease caused by the membrane insertion of p25 was larger than that caused in PC membranes. Alternatively, in the presence of phloretin, the decrease in the potential caused by the peptide insertion was smaller. Complementary studies involving attenuated total reflectance-Fourier transform infrared spectroscopy of the peptide membrane interactions have shown that modification of the dipole potential affects the conformation of the peptide during the course of its interaction with the membrane. The presence of KC induces a higher amount of helicoidal structure. The presence of phloretin, however, does not appear to affect the secondary structure of the peptide. The differences observed in the dipole potential decreases caused by the presence of the peptide with the PC membranes and phloretin-PC membranes, therefore, must involve differences in the tertiary and, perhaps, quaternary conformations of p25.

INTRODUCTION

The membrane dipole potential constitutes, together with the transmembrane potential difference and the membrane surface potential, the set of electrical potentials associated with cell membranes. Although the transmembrane potential and the surface potential have been implicated in the interaction of macromolecules and membranes (see, e.g., McLaughlin, 1989), very little is known about the influence of the dipole potential on such interactions. The membrane dipole potential appears to have its origins in the dipole moments of polar groups from the lipidic components of the bilayer and from water molecules in the transition region between the phases (Brockman, 1994). The dipolar groups are thought to be oriented in a way that the hydrophobic interior of the membrane is positive with respect to the external aqueous phases and has a magnitude of several hundred millivolts.

To date, the thermodynamic potential of membrane dipoles has been shown to influence the translocation of hydrophobic ions through lipidic bilayers (Franklin and Cafiso, 1993). It has also been found that preparation of phospholipid membranes supplemented with a number of different sterols causes changes in the dipole potential in a controlled manner. Thus phloretin, a sterol that significantly reduces the magnitude of the positive dipole potential, was found to increase the translocation rate of hydrophobic cations while decreasing the rate for anions. On the other hand, 6-ketocholestanol (KC), which increases the positive membrane dipole potential, affects the translocation rates of hydrophobic ions in a direction opposite that of phloretin. The interesting possibility also exists, therefore, that such membrane dipoles may also affect the interactions of proteins with membranes and perhaps the properties of protein within membranes. Up to now, however, there have been few studies to address these phenomena (although see Keinker et al., 1994; Bedlack et al., 1994; Zhang et al., 1996; Rokitskaya et al., 1997).

Over the past two decades a series of potentiometric fluorescent indicators that function by putative electrochromic mechanisms have been developed (Loew et al., 1979). The use of these dyes has been successfully applied to the measurement of the membrane potential (Montana et al., 1989; Loew et al., 1992) by a dual-wavelength ratiometric fluorescence method. Recently it has been shown that following this method, the potential sensitive dye 1-(3-sulfonatopropyl)-4-[β[2-(di-n-octyl-amino)-6-naphthyl]vinyl] pyridinium betaine (di-8-ANEPPS) may be used to measure changes in the membrane dipole potential produced by dipolar compounds such as phloretin or KC (Gross et al., 1994; Clarke and Kane, 1997; Clarke, 1997). The dual-wavelength ratiometric method forestalls problems arising from small differences in dye concentration between different samples or dye bleaching, or from the influence of light scattering on the fluorescence measurements.

Received for publication 17 November and in final form 25 January 1998.
Address reprint requests to Dr. Paul O'Shea, The Welsh School of Pharmacy, Redwood Building, King Edward VII Avenue, Cardiff University, Cardiff CF1 3XF, Wales. Tel.: 44-1222-874781; Fax: 44-1222-874149; E-mail: osheaps@cardiff.ac.uk.

0006-3495/98/05/2434/09 $2.00

In the present study we have utilized di-8-ANEPPS to report changes in the dipole potential during the interactions of a typical amphipathic peptide with membranes. This peptide is known as p25 and is the signal sequence of subunit IV of cytochrome *c* oxidase. We have previously studied the interactions of this peptide with membranes by utilizing another fluorescent technique that reports changes in the membrane surface potential (Golding et al., 1996). Thus, by binding and consequent (much slower) membrane insertion of the peptide, small changes in the membrane surface potential take place, which are monitored by changes in the fluorescence of a surface-located fluorescent indicator (Wall et al., 1995; Golding et al., 1996). We have also utilized this technique to study the effect of changing the membrane dipole potential on the interactions of p25 with membranes. Both techniques, involving application of the respective fluorescent probes, were also augmented by studies of peptide membrane interactions using attenuated total reflectance-Fourier transform infrared (ATR-FTIR) spectroscopy. The results of these studies implicate membrane dipole potential as an influential parameter in the membrane insertion and folding of amphipathic peptides.

MATERIALS AND METHODS

All chemical reagents were of the highest purity commercially available. Egg phosphatidylcholine (PC) was obtained from Lipid Products (Cambridge, UK). Phloretin and 6-ketocholestanol (KC) were obtained from Sigma. The leader sequence of the nuclear encoded subunit IV of mammalian cytocrome *c* oxidase (EC 1.9.3.1) was purchased in pure form from Peptide Products (Cambridge, UK). The fluorescent dye di-8-ANEPPS was purchased from Molecular Probes. Fluoresceinphosphatidylethanolamine (FPE) was prepared as previously described (Wall et al., 1995).

Preparation of phospholipid vesicles labeled with either di-8-ANEPPS or FPE

Monodisperse, 100-nm-diameter unillamelar phospholipid vesicles were prepared by a pressure extrusion method as previously described (Wall et al., 1995). Phospholipid (in chloroform/methanol), di-8-ANEPPS (in ethanol) when required, and the appropriate additive (6-ketocholestanol or phloretin in methanol) were mixed in a round-bottomed flask and dried under a stream of oxygen-free argon gas by rotatory evaporation until a thin film was formed. The lipid film was rehydrated with 1 ml of 280 mM sucrose supplemented with 5 mM Tris, pH 7.5, at room temperature. The resulting multilamellar solution was frozen and thawed five times and finally extruded 10 times (Lipex BM Inc., Vancouver, Canada) through 25-mm-diameter polycarbonate filters with a 100-nm pore size (Nucleopore Filtration Products, Pleasonton, CA). This results in a monodisperse, unilamellar supension of phospholipid vesicles.

Liposomes were labeled with FPE as previously described (Wall et al., 1995): briefly, 0.25 mol% equivalent of FPE was placed in a 1.5-ml Eppendorf tube and dried under a stream of argon gas, followed by resolvation with 5 μl of 95% ethanol. This was added to previously prepared liposome suspensions. The mixture was then incubated for 30–60 min in the dark at 37°C. Unincorporated FPE was removed by size exclusion chromatography on a Sephadex PD-10 column.

Fluorescence measurements

Fluorescence spectra and dual-wavelength recordings were obtained on a Shimadzu RF5001 spectrofluorophotometer. Excitation spectra were collected with the emission wavelength at 580 nm (near the emission maximum). The variation of the fluorescence ratio $R(460/520)$ as a function of p25 concentration was measured in the dual-wavelength excitation mode. For each peptide concentration, the data were monitored over a period of 350 s, in which fluorescence was measured for the two-excitation wavelengths every 10 s. In the interval between measurements, the sample was not irradiated, to minimize photobleaching. The lipid concentration was typically 200 μM, and all experiments were performed at room temperature.

The data obtained from the measurement of $R(460/520)$ as a function of p25 concentration were fitted to a simple hyperbolic function, which describes a single binding site model according to

$$R(460/520) = \text{capacity} \cdot [\text{p25}]/K_d + [\text{p25}] \quad (1)$$

where K_d is the dissociation constant and the capacity corresponds to the maximum value of $R(460/520)$.

Time resolution of p25 interactions with phospholipid vesicles

Phospholipid vesicles labeled with either FPE or di-8ANEPPS were subjected to fluorescence investigation with an Applied Photophysics DX-17 MV (Leatherhead, England) stopped-flow mixing apparatus. The measured dead time of this apparatus is 1 ms. For dual-wavelength recordings, the time-dependent fluorescent variation was measured by exciting the dye at two different wavelengths, 460 and 520 nm, and using an optical filter with a 570-nm cutoff to collect the emitted light and process it, as suggested by Gross et al. (1994) and Clarke and Kane (1997).

The lipid concentration for the kinetic measurements was 200 μM, and the p25 concentration was 15 μM. Measurements were performed at room temperature. The resultant time courses of the fluorescence ratio R were best described by

$$R = A \cdot e^{-kt} + \text{offset} \quad (2)$$

where A is the amplitude of the fluorescence change and k is the pseudo-first-order rate constant of the process.

The use of FPE to determine peptide-membrane interactions was performed as previously described (Golding et al., 1996): briefly, FPE-phospholipid vesicles were subjected to stopped-flow measurements with a single excitation wavelength of 490 nm and emitted light recorded above 500 nm. The PC concentration for the FPE measurements was typically 214 μM, and the p25 concentration was 0.6 μM. The various components of the data (e.g., the binding and insertion phases) were found to be described independently by

$$\text{observed signal} = A_1 \cdot e^{-k_1 \cdot t} + A_2 \cdot e^{-k_2 \cdot t} + \text{offset} \quad (3)$$

where A_1 and A_2 are the amplitudes and k_1 and k_2 are the rate constants of the biexponential process.

ATR-FTIR measurements

For infrared spectroscopy, phospholipid vesicles (with 15 mol% phloretin or 6-ketocholestanol or pure PC, as appropriate) were prepared as described above, but using D_2O-based media containing 280 mM sucrose, 10 mM Tris, pD 7.5. Solutions of p25 were prepared in the same medium. One hundred microliters of media containing p25 (110 μM) plus liposomes at 0.9 mM lipid were placed in a SeZn plate (SpectraTech contact sampler HATR) for ATR data acquisition.

ATR infrared spectra were acquired on a Nicolet Impact 410 spectrometer equipped with a DGTS detector, working at an instrumental resolution of 2 cm^{-1}. A total of 1000 scans were averaged at room temperature, apodized with a triangle function, and Fourier-transformed. To obtain the pure spectra of the protein, spectra of the solvent were collected under identical conditions, and subtractions were done with the computer. Residual water vapor bands were also subtracted with a water vapor spectrum.

Infrared spectra were deconvolved using the programs developed by Moffatt et al. (1986), using a half-bandwidth of 25 cm^{-1} and a *k* factor of 2.5. The criteria for setting the deconvolution parameters avoided the appearance of negative side-lobes and mathematical noise. To measure the relative areas of the amide I band components (between 1600 and 1700 cm^{-1}), deconvolved spectra were curve-fitted by means of a least-squares iterative program using a Gaussian bandshape (Byler and Susi, 1986). The peak positions, heights, and bandwidths were allowed to vary simultaneously until a satisfactory fit was achieved. The standard error for the values of the band areas obtained from the iterative curve-fitting of the deconvolved spectra was ~1%.

Being aware of the problems that can arise from the curve-fitting of the deconvolved spectra due to the distorsion of the bandwitdths that may be introduced by the deconvolution procedure (Surewicz and Mantsch, 1988), we further assessed the validity of the fitted bands by comparing the band parameters derived from the fitting process with the characteristic of the fourth-derivative spectra. In the case of p25 interacting with PC membranes and PC-phloretin membranes, for which very similar curve-fitting results were obtained (see Table 4), the fourth-derivative spectra were found to be very similar. For p25 interacting with PC-KC membranes, however, clear differences were observed in the fourth-derivative spectra: the bands at 1659 and 1632 cm^{-1} (α-helix and β-structure, respectively) were clearly less intense than the corresponding bands for the p-25 with PC and PC-phloretin membranes. Because the intensity of the bands in the fourth-derivative spectra is very sensitive to the bandwith of the original band (broad bands give less intense peaks than narrow bands), the decreased intensity of the bands mentioned above is consistent with the increased bandwidth for these two bands (with just a small difference in intensity) obtained from the fitting of the deconvolved spectrum in the case of PC-KC membranes (see Fig. 7). Thus the comparison of the curve-fitting results with the fourth-derivative spectra supports the quantification of the secondary structure and the differences observed.

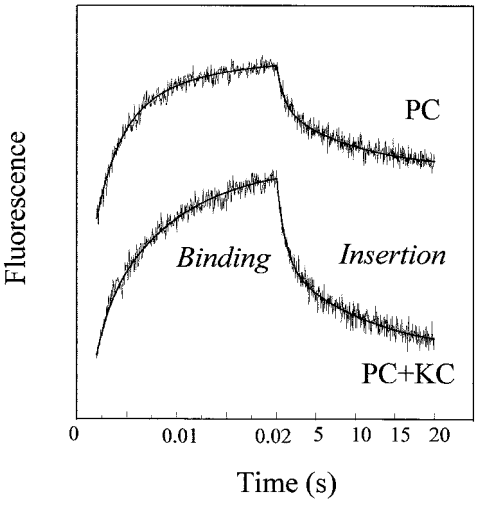

FIGURE 1 Interaction of p25 with FPE-labeled membranes. FPE-labeled phospholipid vesicles (214 μM PC) in 280 mM sucrose, 10 mM Tris, at pH 7.5 were stopped-flow-mixed with p25 (0.6 μM) in the same medium. *Upper trace*: PC vesicles. *Lower trace*: PC vesicles containing 9 mol% KC. The traces cover two time periods (0–0.02 and 0.02–20 s). Each trace represents the average of three independent experiments. The components of the traces labeled Binding and Insertion were independently fitted to Eq. 3. The resultant theoretical fits, excluding the instrumental dead time and flow period, have been drawn as solid lines through the data points.

RESULTS

Interaction of p25 with FPE-labeled vesicles

Fig. 1 illustrates the typical fluorescence changes associated with the stopped-flow mixing of a model amphiphilic peptide (Met-Leu-Ser-Leu-Arg-Gln-Ser-Ile-Arg-Phe-Phe-Lys-Pro-Ala-Thr-Arg-Thr-Leu-Cys-Ser-Ser-Arg-Tyr-Leu-Leu) known as p25, with PC membranes labeled with FPE. The fluorescence yield of this fluorophore has been shown to respond to the addition or loss of net electrical charge at the membrane surface (Golding et al., 1996). The initial increase in fluorescence (0–20 ms) shown in Fig. 1 has been assigned to the binding of the oligopeptide to the membrane surface (Wall et al., 1995; Golding et al., 1996). This fluorescence enhancement is followed by a subsequent, much slower decay (20 ms–20 s) indicating loss of positive charge from the membrane surface, and represents the partial membrane insertion of p25. Both the rapid initial process (labeled *binding* in Fig. 1) and the subsequent decay (labeled *insertion*) comprise two phases and may be fitted to the sum of two exponentials, yielding two rate constants for the binding phase and two for the insertion phase (see Materials and Methods). Iterative fitting (by least squares) of the data shown in Fig. 1 to Eq. 3 yielded values for the rate constants of ~400 and 100 s^{-1} for the binding process and 1 and 0.1 s^{-1} for the insertion process, and are consistent with those previously published (Golding et al., 1996).

Fig. 1 also shows the effects on the fluorescence change of the interaction of p25 with PC membranes containing 9 mol% KC, a compound that is known to increase the dipole potential (Franklin and Cafiso, 1993). The presence of KC has a profound effect on both the binding and insertion processes compared to PC membranes. Analysis of the kinetics of these processes, however, indicates that although there are clearly differences in the extent of the peptide-membrane reaction, the rates are fairly similar. Nevertheless, a change in the dipole potential appears to have a profound effect on the interaction of p25 with lipidic membranes. This observation, therefore, prompted a more detailed study of the relationship between the peptide-membrane interactions and the dipole potential, which involved the application of the fluorescent dye di-8-ANEPPS, which has been shown to be sensitive to variations in this electric potential (Gross et al., 1994), and a comparison of the results to studies that offer more structural details, such as ATR-FTIR spectroscopy.

Fluorescence excitation spectra of di-8-ANEPPS-labeled vesicles

Fig. 2 shows the excitation spectra of phospholipid vesicle suspensions labeled with 4 μM di-8-ANEPPS; spectra of PC liposomes with those obtained containing 15 mol% of either KC or phloretin are compared. Significant variations in the intensity and position of the excitation maximum were observed when these sterols are incorporated into the lipidic bilayer. Montana et al. (1989) have pointed out that such intensity variations may be due in part to a potential-dependent shift in the emission spectrum, which causes a

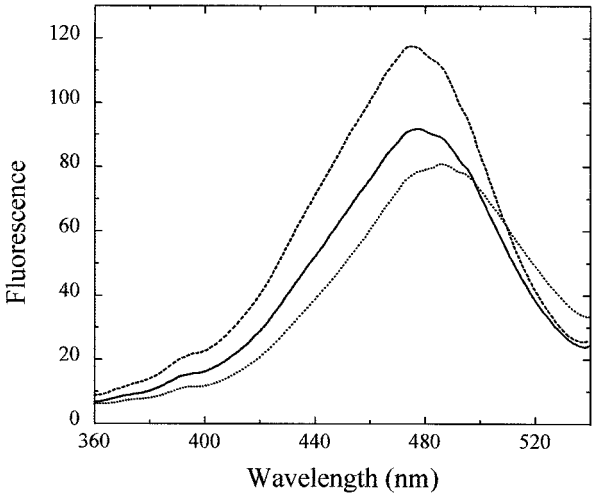

FIGURE 2 Excitation spectra (λ_{em} = 580 nm) of PC (——), PC-KC (KC 15 mol%) (– – –), and PC-phloretin (phloretin 15 mol%) (·····) liposomes labeled with 4 μM di-8-ANEPPS. The lipid concentration was 200 μM.

change in intensity at the fixed emission wavelength used for the excitation scan. These authors demonstrated, however, that the intensity changes may contain other artifactual contributions due to a direct interaction between the dye and some of the compounds used in the experiment.

To determine the changes resulting only from the spectral shift, the areas of the excitation spectra were normalized to the same integrated intensity and then subtracted (Montana et al., 1989). This procedure yields the difference spectra shown in Fig. 3, which were obtained by subtracting the PC-liposome spectrum from the PC-phloretin liposome spectrum, which shows a minimum at 450 nm and a maximum at 520 nm. The presence of KC, however, yields a difference spectrum with a maximum at 450 nm and a minimum at 520 nm, which is the opposite of the effect of phloretin. Recording the ratio (*R*) of fluorescence excited at the two wavelengths with the maximum positive and negative changes provides a method, therefore, for measuring spectral shifts originated by changes in the local electric field, avoiding the artifactual variations in intensity. The feasibility of measuring the membrane dipole potential by measuring *R* has been explored by other laboratories (Montana et al., 1989; Loew et al., 1992), and the possibility of using the ratiometric method to measure variations of the membrane dipole potential has been reported by Gross et al. (1994), Clarke and Kane (1997), and Clarke (1997). In agreement with these results, the data shown in Fig. 3 are consistent with an increase in the membrane dipole potential caused by the presence of KC and a decrease caused by phloretin, i.e., a respective increase and decrease in the ratio *R*. The values of *R* obtained by measuring the fluorescence at two excitation wavelengths, 460 and 520 nm (λ_{em} = 580 nm), are shown in Table 1 for the different membrane systems used throughout the remainder of this study.

To rule out the possibility of changes in the surface electrostatic potential that may conceivably influence the

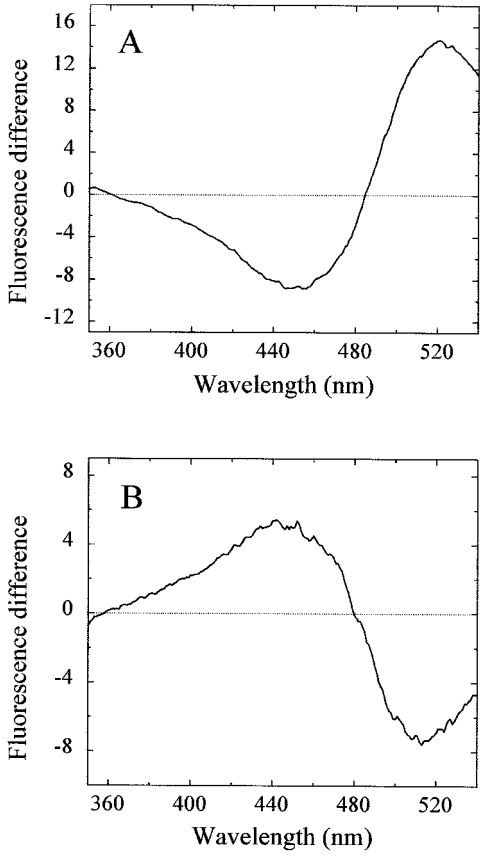

FIGURE 3 Di-8-ANEPPS-labeled liposome fluorescence difference spectra. (*A*) Excitation spectrum of PC-phloretin (phloretin 15 mol%) liposomes minus excitation spectrum of PC liposomes. (*B*) Excitation spectrum of PC-KC (KC 15 mol%) minus excitation spectrum of PC liposomes. Before subtraction the spectra were normalized to the integrated areas so that the difference spectra would reflect only spectral shifts. The dye concentration was 4 μM. The lipid concentration was 200 μM. λ_{em} = 580 nm.

response of the dye, the effect of adding $CaCl_2$ (Wall et al., 1995) to a suspension of di-8-ANEPPS-labeled liposomes was investigated. The resultant difference spectrum was obtained between 350 and 560 nm as before, and indicated that changes in the surface potential do not interfere with the spectroscopic properties of di-8-ANEPPS.

TABLE 1 Values of the fluorescence ratio *R*(460/520) for the different membrane systems used

Membrane system	*R*(460/520)
PC-KC 15 mol%	4.080
PC	3.191
PC-phloretin 5 mol%	2.699
PC-phloretin 15 mol%	1.955

R was determined from the ratio of the values of the fluorescence measured at 580 nm from the two different excitation wavelengths, 460 and 520 nm. The lipid concentration in the liposome suspensions used for the measurement of *R* was 200 μM.

Influence of the interaction of p25 on the membrane dipole potential, as revealed by changes in the fluorescence of di-8-ANEPPS

The same kind of approach as that described above has been applied to the study of the interaction of p25 with lipidic membranes and the effects that the variation in the membrane dipole potential (attained by incorporating into the lipidic bilayer either phloretin or KC; see Table 1) has on the interactions. Fig. 4 displays the difference spectra obtained by subtracting the PC-liposome spectrum from the spectrum of a suspension containing PC-liposomes and 15 μM p25. The interaction of p25 with the membrane promotes a redshift in the excitation spectra that results in a difference spectrum very similar to, although less intense than that obtained with 15 mol% phloretin (Fig. 3 *A*), with a minimum between 450 and 460 nm and a maximum at ~520 nm. Thus the interaction of p25 with the PC membrane causes a decrease in the ratio *R*(460/520) and hence promotes a decrease in the membrane dipole potential.

Variation in *R*(460/520) as a function of p25 concentration

The variation in *R*(460/520) as a function of p25 concentration for the different membrane systems shown in Table 1 is displayed in Fig. 5. For the sake of clarity, the value of *R*(460/520) without p25 present was set to 1 (i.e., 100%) for all of the membrane systems. It was observed (Fig. 5) that in all cases, p25 causes a decrease in *R*(460/520). Nevertheless, the magnitude of this decrease depends on the initial characteristics of each membrane system (i.e., the amount of KC or phloretin present in the membrane). Clarke and Kane (1997) reported that di-8-ANEPPS shows significant temperature-dependent shifts in its excitation spectra. This may be indicative of a direct effect of membrane fluidity changes on the fluorescence yield of the dye when measured near the emission maximum. These authors suggest, however, that the influence of such fluidity effects on *R* may be avoided by measuring the fluorescence at the red edge of the emission spectra. The fact that the measurement of *R* in our studies gave the same result when the emission wavelength was set near the emission maximum (580 nm) and when it was set at the red edge of the emission spectra (630 nm), however, shows that no fluidity changes of the kind described by Clarke and Kane (1997) are detected in our case.

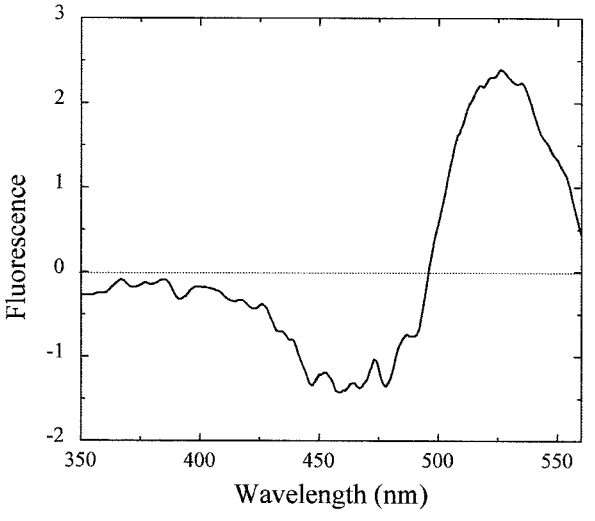

FIGURE 4 Fluorescence difference spectra obtained by subtracting the excitation spectrum of PC lipsomes from the excitation spectrum of PC liposomes plus p25. Before subtraction the spectra were normalized to the integrated areas so that the difference spectra would reflect only spectral shifts. The dye concentration was 4 μM. The lipid concentration was 200 μM. λ_{em} = 580 nm.

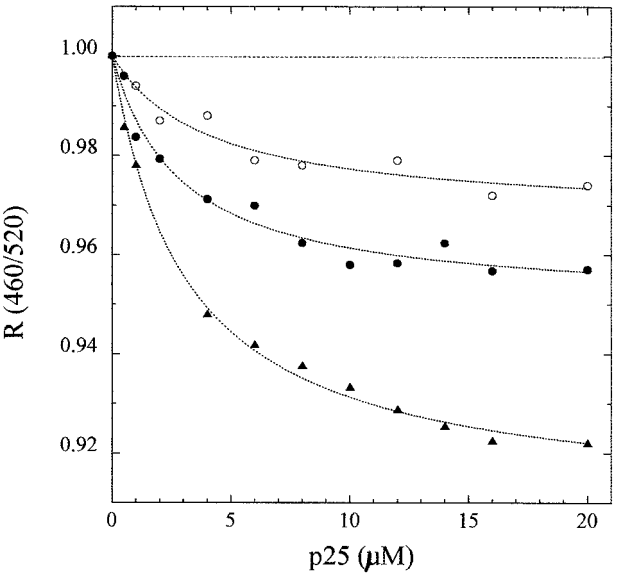

FIGURE 5 Variation of the fluorescence ratio *R*(460/520) as a function of p25 concentration. ▲, PC-KC liposomes (KC 15 mol%); ●, PC liposomes; ○, PC-phloretin liposomes (5 mol% phloretin). The lipid concentration was 200 μM. The fitting of the data to Eq. 1 is shown (·····).

Each data set in Fig. 5 was fitted to Eq. 1 (see Materials and Methods), which implies that p25 binds to a single population (or type) of binding site. The binding affinity and apparent abundance of these sites are described more fully in Table 2. The values calculated for the dissociation constants (K_d around 3–4 μM) are in excellent agreement with the K_d values previously described by different methods (Golding et al., 1996; Swanson and Roise, 1992).

There were no apparent influences of the presence of phloretin or KC on the thermodynamic affinity of the bind-

TABLE 2 Dissociation constants and capacity derived from the fitting of the variation of *R* with p25 concentration (Fig. 5) to Eq. 1 for PC liposomes and PC liposomes containing 5 mol% phloretin and 15 mol% KC

	K_d (μM)	Cap
PC-KC (15 mol%)	3.1 ± 0.2	−0.090 ± 0.002
PC	2.8 ± 0.5	−0.049 ± 0.002
PC-PHL (5 mol%)	4.0 ± 1.1	−0.032 ± 0.003

ing of the peptide for each membrane system. On the other hand, the *capacity*, a parameter that reflects the maximum extension of the variation of *R* in each case and is interpreted to indicate the extent of binding, clearly depends on the presence of the compounds that modify the membrane dipole potential. The reduction in *R* is larger than that in PC when KC is present in the membrane. In contrast, the decrease in *R* is smaller than that in PC when phloretin is present. Thus Fig. 5 shows that the larger the initial positive membrane dipole potential, the larger is the decrease in the dipole potential caused by the interaction of the peptide with the membrane.

Time evolution of the dipole potential during the interaction of p25 with the membrane

The foregoing results characterize the relationship between the interaction of p25 with the membrane and the membrane dipole potential at the equilibrium state. To obtain information about the kinetics of these processes, fluorescence stopped-flow mixing experiments were carried out with the aim of measuring the time course of *R*(460/520) within the millisecond time domain. No variations in *R* were detected in the millisecond time domain. However, the variation in the fluorescence ratio, detected in the seconds time scale, is shown in Fig. 6. The experimental traces were fitted to a single-exponential process (Eq. 2); the corresponding rate constants and amplitudes are summarized in Table 3.

In good agreement with the data presented in Fig. 5, it was observed that *R*(460/520) decreases when p25 interacts with the membrane, and the amplitude of the decrease is larger for 15 mol% KC-PC membranes and smaller for 15 mol% phloretin-PC membranes, compared to similar experiments with 100% PC membranes. Thus the rate constants of these processes appear to be sensitive to the initial value of the membrane dipole potential. These data indicate that the lower the initial membrane dipole potential, the slower is the variation of the membrane dipole potential induced by the interaction of the peptide. The magnitude of the rate constant is comparable to the slower of the two rate constants of the peptide insertion process shown in Fig. 1. It is also worth emphasizing that this latter rate constant has been implicated to indicate the rate of folding of the peptide within the membrane (Golding et al., 1996)

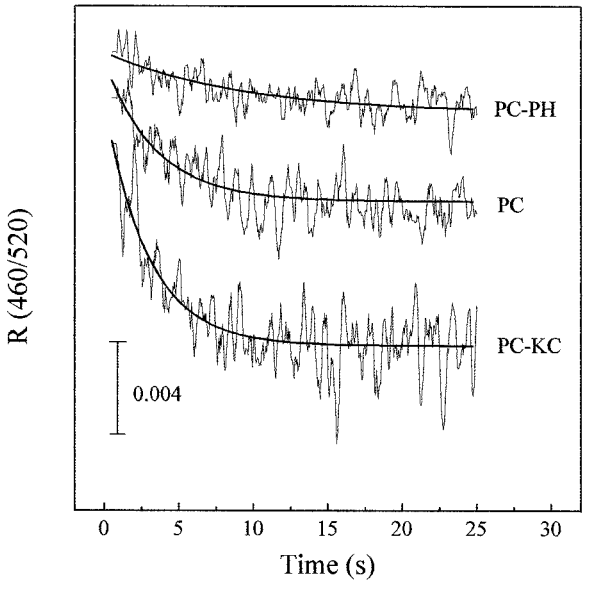

FIGURE 6 Time course variation of the ratio *R*(460/520), measured with the stopped-flow technique. The molar ratio of sterol in PC-phloretin (PC-PH) and PC-KC liposomes was 15 mol%. The lipid concentration was 200 μM. The p25 concentration was 15 μM.

TABLE 3 Rate constants and amplitudes derived from the fitting of the time course variation of *R* (Fig. 6) to Eq. 2 for PC-liposomes and liposomes containing 15 mol% phloretin or KC

	k (s^{-1})	Amplitude
PC-KC (15 mol%)	0.34 ± 0.10	0.0108 ± 0.0010
PC	0.29 ± 0.12	0.0061 ± 0.0009
PC-PHL (15 mol%)	0.11 ± 0.04	0.0027 ± 0.0005

Influence of the membrane dipole potential on the secondary structure of p25

Fig. 7 *A* compares the deconvolved spectrum of p25 in aqueous solution with the spectrum obtained in the presence of PC vesicles. The resolved peaks can be related to different secondary structures according to previous assignments described in the literature (Byler and Susi, 1986; Surewicz and Mantsch, 1988). The FTIR spectrum of p25 shows a broad band with a maximum centered at 1645 cm^{-1}. This indicates that the structure of the peptide is mainly unordered. The shoulder at 1615 cm^{-1} lies in a region in which bands have been observed for some synthetic peptides that form an intermolecular network of hydrogen-bonded β-sheets (Surewicz et al., 1987). Two other very smooth shoulders can be distinguished around 1665 and 1675 cm^{-1} and can be assigned to peptide turns. In the presence of PC phospholipid vesicles, the 1615 cm^{-1} band completely disappears, and four structural components can be identified after the deconvolution procedure. The shoulder around 1625 cm^{-1} and the peaks at 1645 and 1675 cm^{-1} correspond to β-structure, unordered structure, and turns, respectively. The peak at 1658 cm^{-1} lies in the upper edge of the region in which bands corresponding to helical structure usually appear. In most cases the typical α-helical structure displays a somewhat lower IR frequency in D_2O (~1653 cm^{-1}). This unusually high frequency may be associated with a distortion of the helices, as bands around 1660 cm^{-1} have previously been associated with such phenomena (Krimm and Bandekar, 1986; Muga et al., 1990). The formation of such helical structures of p25 located within membranes is in good agreement with previous studies (Tamm and Bartoldus, 1990; Golding et al., 1996).

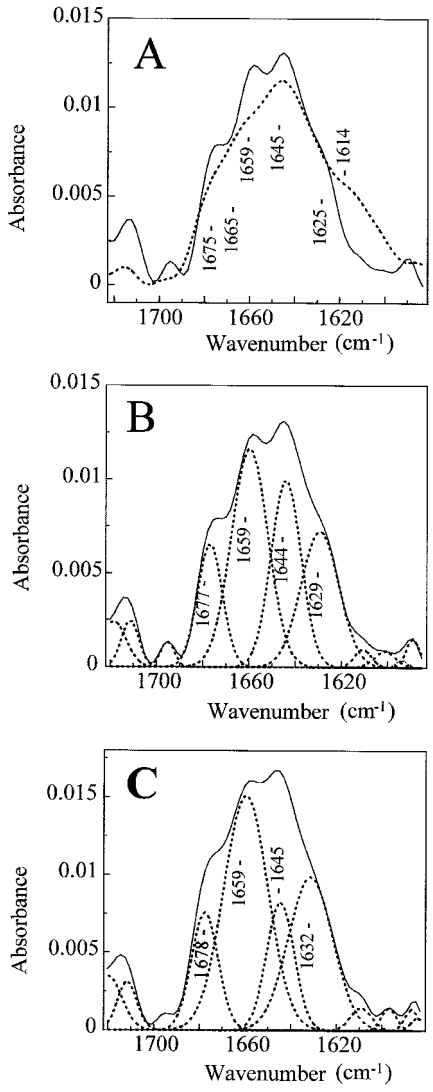

FIGURE 7 ATR-FTIR spectra of p25 in solution and in the presence of PC and PC-KC membranes. (*A*) Fourier self-deconvolved spectra (amide I region) of p25 (112 μM) in D_2O buffer (·····) and p25 (112 μM) plus PC (900 μM) membranes in the same buffer (——). The best fitted individual component bands for the deconvolved spectra of p25 in the presence of PC membranes (*B*) and PC membranes containing 15 mol% KC (*C*) are shown. Some bands that do not correspond to the amide I region were included in the curve fittings to avoid the need for a baseline correction. The original spectrum and the result of the curve fitting are indistinguishable. Deconvolution parameters: FWHH = 25, k = 2.5.

Infrared spectra of p25 interacting with PC membranes in the presence of phloretin or KC (PC/compound = 15 mol%) were also obtained and Fourier self-deconvolved. To quantify the different types of secondary structure and to assess the influence of the dipolar compounds, curve-fitting was performed over the deconvolved spectra. Fig. 7, *B* and *C*, shows the best-fitted individual bands for the deconvolved spectra of p25 in the presence of PC membranes and PC-KC membranes at a KC/PC molar ratio of 15%. The influence of the different dipolar compounds on the peptide secondary structure is summarized in Table 4. It can be inferred from this table that the presence of the dipolar compounds does not alter the number and position of peaks in the IR spectrum. Nevertheless, important differences were found for the calculated amounts of the different secondary structure types. Although the secondary structures of the peptide in the presence of PC vesicles and PC-phloretin vesicles are very similar, the presence of 15 mol% KC caused a significant increase in the helical and β-structure content. The extent of unordered structures was reduced in the presence of PC-KC membranes.

TABLE 4 Effect of the dipolar compounds on the secondary structure of p25

	Helix	Beta	Unordered	Turns
PC	1659 (37%)	1629 (24%)	1644 (26%)	1677 (14%)
PC-PHL	1659 (38%)	1629 (22%)	1644 (28%)	1677 (13%)
PC-KC	1659 (44%)	1632 (30%)	1645 (14%)	1678 (12%)

Positions, fractional areas, and assignments of the amide 1 bands of samples containing p25 in the presence of PC membranes (PC), and p25 in the presence of PC membranes with 15 mol% phloretin (PC-PHL) or KC (PC-KC). The component bands were obtained by curve-fitting the deconvolved spectra as shown in Fig. 7. Frequency positions are expressed in cm^{-1}. The numbers in brackets express the percentage of amide I that corresponds to each component band.

DISCUSSION

The dual-wavelength fluorescence ratiometric technique of di-8-ANEPPS, combined with the use of dipolar compounds and infrared spectroscopy, has facilitated the study of the influence of the dipole potential on the interaction of the signal sequence p25 with lipidic membranes and the effects of dipole potential variations on the secondary structure of the peptide.

Franklin and Cafiso (1993) showed that the effect of phloretin and KC on the membrane permeability to hydrophobic ions can be accounted for by a simple model that treats such effects as a result of global electrostatics, whereas other nonelectrostatic changes that may be produced by phloretin and KC (changes in lipid acyl chain packing and in the headgroup structure, specific interaction with the hydrophobic ions) are negligible. Consistent with this, structural studies by Bechinger and Seelig (1991) found no evidence that phloretin significantly alters the acyl chain order of the lipid packing of the membrane. On the other hand, it has been shown that KC does not modify the bilayer thickness, but does produce a much smaller increase in the compressibility modulus than does cholesterol and produces much smaller changes in the acyl chain order (Simon et al., 1992; Franklin and Cafiso, 1993).

Fluorescence difference spectra of di-8-ANEPPS-labeled liposomes containing phloretin or KC and the fluorescence ratio R(460/520) derived from the dual-wavelength measurements for these membrane systems in sucrose buffer (Fig. 3) are in agreement with previous data reported in the literature (Gross et al., 1994). Phloretin, which is known to decrease the membrane dipole potential, causes a redshift of

the excitation spectra of the dye and gives a ratio *R* that is lower than that of PC membranes. On the other hand, when KC is incorporated into the bilayer, the opposite effect is observed (a blueshift and an increase in *R*). According to Gross et al. (1994), the changes in *R* reflect the variation in the dipole potential, and the ratio is insensitive to changes in the membrane's viscosity and to changes in the surface potential.

The fluorescence difference spectra that resulted from the interaction of p25 with PC membranes showed that the peptide decreases the dipole potential of the membrane. Moreover, the variation in *R* as a function of p25 concentration, detected with PC vesicles, in which the dipole potential was modified by the presence of phloretin or KC, showed that the reduction in the dipole potential caused by the peptide increases as the initial positive value of the membrane dipole potential increases. The larger the initial *R* value of the membrane, the larger the decrease in *R* induced by the interaction of the peptide. The relationship between the measured variations in the dipole potential and the interaction of the peptide with the membrane was underlined by the good agreement between the dissociation constants calculated from the fitting of data in Fig. 5 and the dissociation constants derived from binding curves by complementary techniques (Wall et al., 1995).

The kinetic studies revealed that when p25 and PC-vesicle suspensions were mixed, *R* was found to decrease, following a process best described as monoexponential. The amplitude of the process appears to depend on the initial value of the membrane dipole potential, consistent with the results derived from the experiments at equilibrium discussed above. The rate constants calculated from the fluorescence traces (between 0.1 and 0.3 s^{-1}) are comparable to the rate constants of the membrane insertion process of p25 shown in Fig. 1 (see also Golding et al., 1996). This comparison leads to the conclusion that the variation in the dipole potential induced by the peptide and the effect that the dipole potential exerts on the membrane-peptide interaction take place during the insertion process of the peptide into the membrane, rather than during the initial membrane-binding event.

The secondary structure characterization derived from the infrared spectra (Fig. 7) indicated that the variations in the membrane dipole potential result in differences in the conformation of the peptide. It is shown in Fig. 5 that when KC was present in the membrane, the interaction of the peptide induced a larger decrease in the dipole potential and adopted a structure with a higher degree of α-helical content compared to that of PC liposomes. On the other hand, when phloretin was present, no secondary structural changes were observed with respect to PC membranes, despite the fact that the interaction of the peptide reduced the dipole potential. This reduction may then be caused by variations in the tertiary and/or quaternary conformation of the peptide. Cafiso (1991) pointed out, for example, that the folding of a hydrophobic portion of the peptide into two antiparallel helices could overcome the energetically unfavorable insertion of the amino terminal of an α-helix (because of the interaction of the membrane dipole with the helix dipole). This kind of contact could also arise from helices from different peptide monomers. Another possibility may be considered: when an α-helix inserts into the membrane, the magnitude of the dipole potential variation induced by the dipole moment of the helix must also depend on the degree of tilting of its axis with respect the membrane normal. It has previously been reported (Goormaghtigh et al., 1989) that in cardiolipin-containing vesicles, p25 forms a helical structure parallel to the acyl chains of the lipids, whereas in pure DOPC vesicles the helix orients much closer to the lipid-water interface. Thus the obliqueness of the helix in the membrane may be a crucial parameter for the degree of membrane destabilization and the promotion of processes such as membrane fusion or protein transport (Brasseur et al., 1997).

The ability of p25 to promote intermembrane contacts has previously been described (Leenhouts et al., 1994; Torok et al., 1994). From the results reported in the present study, no details can be deduced about peptide-peptide or membrane-membrane interactions. The discussion presented above, however, emphasizes the complexity and variety of factors that may be involved and may contribute to the origin and evolution of the membrane dipole variations detected and their influence on the structure of oligopeptides within membranes.

CONCLUSIONS

The combination of the use of a FPE-based technique, the dual-wavelength fluorescence ratiometric method, with di-8ANEPPS and ATR-FTIR spectroscopy to study the relationship between the interaction of the signal peptide p25 with model membranes and the dipole potential has yielded three main conclusions: 1) When the peptide inserts into the membrane, it causes a decrease in the membrane dipole potential. 2) Such a decrease depends on the initial value of the membrane dipole potential (the more positive the initial dipole potential, the larger is the decrease caused by the peptide insertion). 3) The magnitude of the positive membrane dipole potential affects the conformation of the peptide within the membrane. The experimental evidence presented herein therefore emphasizes the importance of the dipole potential in the determination of peptide-membrane interactions. The results should draw attention to the dipole potential and its possibly influential role in the folding of peptide chains within membranes. Such studies may shed further light on the folding mechanisms of nascent integral membrane proteins.

We are grateful to the Ministerio de Educacion y Cultura (Spain) for the award of a postdoctoral fellowship to JC.

REFERENCES

Bechinger, B., and J. Seelig. 1991. Interaction of electric dipoles with phospholipid headgroups. A ^{2}H and ^{31}P NMR study of phloretin and

phlortein analogues in phosphatidylcholine membranes. *Biochemistry*. 30:3923–3929.

Bedlack, R. S., M. D. Wei, S. H. Fox, E. Gross, and L. M. Loew. 1994. Distinct electric potentials in soma and neurite membranes. *Neuron.* 13:1187–1193.

Brasseur, R., T. Pillot, L. Lins, J. Vandekerckhove, and R. Maryvonne. 1997. Peptides in membranes: tipping the balance of membrane stability. *Trends Biochem. Sci.* 22:167–171.

Brockman, H. 1994. Dipole potential of lipid membranes. *Chem. Phys. Lipids.* 73:57–59.

Byler, D. M., and H. Susi. 1986. Examination of the secondary structure of proteins by deconvolved FTIR spectra. *Biopolymers.* 25:469–487.

Cafiso, D. S. 1991. Lipid bilayers: membrane-protein electrostatic interactions. *Curr. Opin. Struct. Biol.* 1:185–190.

Cladera, J., M. Sabes, and E. Padros. 1992. Fourier transform infrared analysis of bacteriorhodopsin secondary structure. *Biochemistry*. 31: 12363–12368.

Clarke, R. J. 1997. Effect of lipid structure on the dipole potential of phosphatylcholine bilayers. *Biochim. Biophys. Acta.* 1327:269–278.

Clarke, R. J., and D. J. Kane. 1997. Optical detection of membrane dipole potential: avoidance of fluidity and dye-induced effects. *Biochim. Biophys. Acta.* 1323:223–239.

Franklin, J. C., and D. S. Cafiso. 1993. Internal electrostatic potentials in bilayers: measuring and controlling dipole potentials in lipid vesicles. *Biophys. J.* 65:289–299.

Golding, C. A., S. Senior, M. T. Wilson, and P. O'Shea. 1996. Time resolution of binding and membrane insertion of a mitochondrial signal peptide: correlation with structural changes and evidence for cooperativity. *Biochemistry*. 35:10931–10937.

Goormaghtigh, E., I. Martin, M. Vandenbranden, R. Brasseur, and J. M. Ruysschaert. 1989. Secondary structure and orientation of a chemically synthesized mitochondrial signal sequence in phospholipid bilayers. *Biochem. Biophys. Res. Commun.* 158:610–616.

Gross, E., R. S. Bedlack, and L. M. Loew. 1994. Dual-wavelength ratiometric fluorescence measurement of the memrbane dipole potential. *Biophys. J.* 67:208–216.

Keinker, P. K., W. F. Degrado, and J. D. Lear. 1994. A helical-dipole model describes the single channel current rectification of an uncharged peptide ion-channel. *Proc. Natl. Acad. Sci. USA.* 91:4859–4863.

Krimm, S., and J. Bandekar. 1986. Vibrational spectroscopy and conformation of peptides, polypeptides and proteins. *Adv. Protein Chem.* 38:181–364.

Leenhouts, J. M., Z. Torok, R. A. Demel, J. De Gier, and B. De Kruijff. 1994. The full length of a mitochondrial presequence is required for efficient monolayer insertion and interbilayer contact formation. *Mol. Membr. Biol.* 11:159–164.

Loew, L. M., L. B. Cohen, J. Dix, E. N. Fluhler, V. Montana, G. Salama, and J.-Y. Wu. 1992. A naphtyl analog of the aminostyryl pyridinium class of potentiometric membrane dyes shows consistent sensitivity in a variety of tissue, cell, and model membrane preparations. *J. Membr. Biol.* 130:1–10.

Loew, L. M., S. Scully, L. Simpson, and A. S. Waggoner. 1979. Evidence for a charge-shift electrochromic mechanism in a probe of membrane potential. *Nature.* 281:497–499.

McLaughlin, S. 1989. The electrostatic properties of membranes. *Annu. Rev. Biophys. Biophys. Chem.* 18:113–136.

Moffat, D. J., J. K. Kaupinnen, D. G. Cameron, H. H. Mantsch, and R. N. Jones. 1986. Computer programs for infra-red spectrophotometry. NRCC Bulletin 18. National Research Council, Ottawa, Canada.

Montana, V., D. L. Farkas, and L. M. Loew. 1989. Dual-wavelength ratiometric fluorescence measurements of membrane potential. *Biochemistry*. 28:4536–4539.

Muga, A., W. K. Surewicz, P. T. T. Wong, V. K. Singh, T. Shinohara, and H. H. Mantsch. 1990. Structural studies with the uveopathogenic peptide M derived from retinal S-antigen. *Biochemistry*. 29:2925–2930.

Rokitskaya, T. I., Y. N. Atonenko, and, E. A. Kotova. 1997. Effect of the dipole potential of a bilayer lipid membrane on gramicidin channel dissociation kinetics. *Biophys. J.* 73:850–854.

Seelig, J., P. M. Macdonald, and P. G. Scherer. 1987. Phospholipid head groups as sensors of electric charges in membranes. *Biochemistry*. 26:7535–7541.

Simon, S. A., T. J. McIntosh, A. D. Magid, and D. Needham. 1992. Modulation of the interbilayer hydration pressure by the addition of dipoles at the hydrocarbon/water interface. *Biophys. J.* 61:786–799.

Surewicz, W. K., and H. H. Mantsch. 1988. New insight into protein secondary structure from resolution-enhanced infrared spectra. *Biochim. Biophys. Acta.* 952:115–130.

Surewicz, W. K., H. H. Mantsch, G. L. Stahl, and R. M. Epand. 1987. Infrared spectroscopy evidence of conformational transitions of an atrial natriuretic peptide. *Proc. Natl. Acad. Sci. USA.* 84:7028–7031.

Swanson, S. T., and D. Roise. 1992. Binding of a mitochondrial presequence to natural and artificial membranes. *Biochemistry*. 31: 5746–4751.

Tamm, L. K., and I. Bartoldus. 1990. Secondary structure of a mitochondrial signal peptide in lipid bilayer membranes. *FEBS Lett.* 272:29–33.

Torok, Z., R. A. Demel, J. M. Leenhouts, and B. De Kruijff. 1994. Presequence mediated intermembrane contact formation and lipid flow. A model membrane study. *Biochemistry.* 33:5589–5594.

Wall, J., C. A. Golding, M. Van Veen, and P. O'Shea. 1995. The use of fluoresceinphosphatidylethanolamine (FPE) as a real-time probe for peptide-membrane interactions. *Mol. Membr. Biol.* 12:183–192.

Zhang, J., L. M. Loew, and R. M. Davidson. 1996. Faster voltage-dependent activation of Na^+ channels in growth cones versus somata of neuroblastoma N1E-115 cells. *Biophys. J.* 71:2501–2508.